

1989

NASA/ASEE SUMMER FACULTY FELLOWSHIP PROGRAM

MARSHALL SPACE FLIGHT CENTER
THE UNIVERSITY OF ALABAMA IN HUNTSVILLE

FREQUENCY RESPONSE OF ELECTROCHEMICAL CELLS

Prepared by:	Daniel L. Thomas
Academic Rank:	Assistant Professor
University and Department:	The University of Alabama in Huntsville Chemical Engineering Program Mechanical Engineering Department
NASA/MSFC:	
Laboratory:	Electronics and Information Systems
Division:	Electrical
Branch:	Electrical/Electronics Parts
MSFC Colleague:	Teddy M. Edge
Date:	August 11, 1989
Contract No.:	The University of Alabama in Huntsville NGT-01-008-021

ACKNOWLEDGEMENTS

I wish to acknowledge the staff of the Electronics Division of the Electronics and Information Systems Laboratory led by Mr. Jim Miller. In particular, I wish to thank Mr. Al Norton, Jr., for helping to round up equipment and fabrication the test cell and reference electrode, Mr. Ted Edge and Mr. Mike Martin for sponsoring me, and Mr. Roy Lanier for supplying some of the equipment used.

FREQUENCY RESPONSE OF POROUS BATTERY ELECTRODES

Daniel L. Thomas
Assistant Professor of Chemical Engineering
The University of Alabama in Huntsville
Huntsville, AL 35899

ABSTRACT

Impedance concepts can be applied to the analysis of battery electrodes, yielding information about the structure of the electrode and the processes occurring in the electrode. Structural parameters such as the specific area (surface area per gram of electrode) can be estimated. Electrode variables such as surface overpotential, ohmic losses and diffusion limitations may be studied.

Nickel and cadmium electrodes were studied by measuring the A.C. impedance as a function of frequency, and the specific areas that were determined were well within the range of specific areas determined from BET measurements by other workers. Impedance spectra were measured for the nickel and cadmium electrodes, and for a 20 A-hr NiCd battery as functions of the state of charge. More work is needed to determine the feasibility of using frequency response as a non-destructive testing technique for batteries.

INTRODUCTION

Electrochemical processes may and have been studied using frequency response techniques and modeled using impedance concepts. Processes that occur at electrodes may be modeled as resistance, capacitance or complex impedance. More information may be gained using dynamic techniques than by using steady-state D.C. techniques. For example, one could study an electrode by measuring steady D.C. current and potential, or the same system could be studied using A.C. over a range of frequencies with an increase in the amount of information learned. Dynamic techniques have been used to estimate the specific area of porous lead-acid battery electrodes (Newman and Tiedemann, 1976), the kinetics and mechanisms of electrode reactions and the rate of mass-transport processes such as diffusion (Bard and Faulkner, 1980). Attempts have been made to correlate cell state of charge with A.C. impedance spectra (Brodd and DeWane, 1963; Sathyanarayana et al., 1979). Zimmerman et al. (1982) studied the very low frequency impedance (as low as 0.1 Hz) of NiCd cells.

OBJECTIVES

The objective of this work was to examine the feasibility of using frequency response techniques 1) as a tool in destructive physical analysis of batteries, particularly for estimating electrode structural parameters such as specific area, porosity and tortuosity and 2) as a non-destructive testing technique for obtaining information such as state of charge and acceptability for space flight. It would be desirable to have a non-destructive battery test that can be run rapidly and as close to launch of spacecraft as possible. The battery frequency response may be such a test.

THEORY

This section will briefly review the physical phenomena that contribute to the frequency response of an electrode.

Electric Double Layer

The double layer is a thin (about 20 Angstrom) layer of electric charge that exists at the boundary between two phases, such as an electrode/solution interface, and can form for several reasons. One of the poles in a polar solvent molecule may be preferentially oriented toward the surface. Figure 1 shows how the negative pole of a water molecule may be oriented toward a surface and create a separation of charge. Double layers also occur because positive or negative ions may be preferentially adsorbed by a surface. For example, chloride ions in a solution of potassium chloride are adsorbed onto mercury in preference to potassium ions as shown in Figure 2, resulting in a separation of charge.

Finally, double layers are formed when electrodes are charged. Consider the situation in Figure 3, where two inert metal surfaces such as gold are immersed in NaF solution. These ions are not preferentially adsorbed by the metal. If a potential difference less than the 1.2 V required to decompose water is placed across the cell no steady state current can flow, yet there must be a potential drop. The potential drop occurs at the double layers that exist at each electrode surface. Electrodes which behave in this way are called ideally polarizable electrodes (IPE).

The double layer can be considered as an electric capacitor since it acts to store charge. The concept of the double layer was experimentally verified with mercury which has the advantage of a reproducible liquid surface and of inhibiting hydrogen evolution and hence approaching IPE

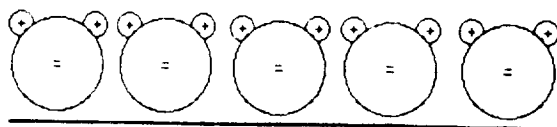


Figure 1. Double layer formation by solvent molecule orientation.

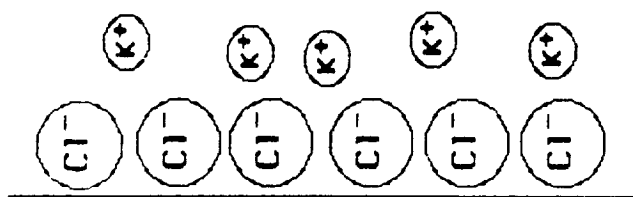


Figure 2. Double layer formation by ion adsorption.

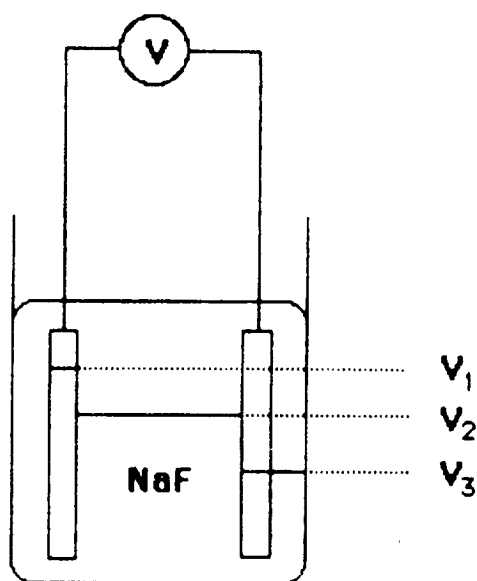


Figure 3. Voltage profile in cell with ideal polarizable electrodes.

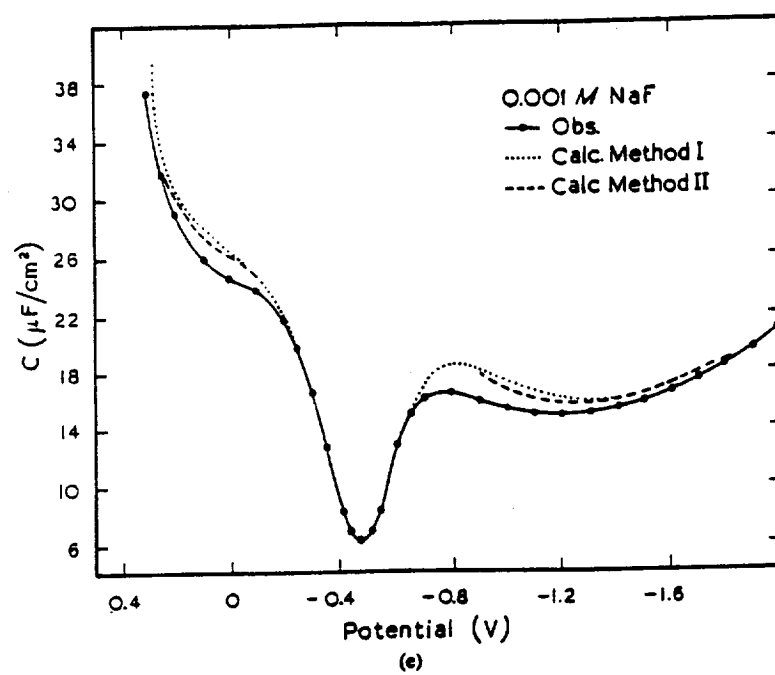


Figure 4. Double layer capacity of 0.001 M NaF/Hg electrode.

behavior over a wide potential range (Newman, 1973). Figure 4 shows how the double layer capacitance of mercury in 0.001 M NaF varies with applied potential. The capacitance was also calculated from the mercury surface tension (which varies with potential and charge) and from direct measurement of charge, both of which require liquid metal electrodes. The double layer capacitance is on the order of $10 \mu\text{F}/\text{cm}^2$, which corresponds to a parallel plate capacitor with a plate separation of about 20 Å, the double layer thickness. The double layer capacitance is potential dependent, but can be treated as constant over small (7 mV) potential range.

Electrochemical Reaction

The rate of electrochemical reaction is an exponential function of the potential drop across the double layer

$$i_f = i_0 \left\{ \exp\left(\frac{\alpha_a F (V_m - V_s)}{RT}\right) - \exp\left(-\frac{\alpha_c F (V_m - V_s)}{RT}\right) \right\} \quad (1)$$

where i_0 is the exchange current density, α is a kinetic symmetry parameter usually taken to be 0.5, F is Faraday's constant, R is the gas constant, T is the absolute temperature and $V_m - V_s$ is the potential drop across the double layer. The first term in brackets is the rate of the forward or anodic reaction while the second term is the rate of the reverse or cathodic reaction. When $V_m = V_s$ then these two rates are equal (to the exchange current density) and there is no net current.

Equation 1 is highly non-linear and must be linearized before using in an impedance analysis:

$$R_f = \left. \frac{d(V_m - V_s)}{di_f} \right|_{(V_m - V_s)^0}$$

Linear expressions are valid for potential variations of 7 mV or less.

Combined Reaction and Double Layer Charging

Most electrodes, particularly those used in batteries, have combined reaction and double layer charging. For a bare metal electrode in contact with solution this can be modeled as a resistor (R_f) and capacitor (C_d) in parallel as shown in Figure 5. The solution resistance R_s also must be considered. At very high frequencies the phase angle is 0 and the modulus of the impedance is R_s , while at sufficiently low frequencies the phase angle is 0 and the modulus is $R_s + R_f$. Hence R_f and R_s can be separately determined, which could not be done readily using a steady D.C. experiment.

Diffusion Effects

Slow diffusion of reactants to the electrode surface or of reaction products away from the surface also causes the potential to lag the current. The Nernst equation, and its linearized form, gives the potential drop due to concentration differences:

$$V_b - V_s = \frac{nF}{RT} \ln \frac{C_s}{C_b} \approx \frac{nF}{RTC_b} (C_b - C_s) \quad (4)$$

where C_b is the bulk solution concentration and C_s is the concentration adjacent to the electrode. Again, the linearization is valid for a potential range of 5-7 mV. Hence, as the reaction proceeds and the reactant near the surface is consumed this potential drop increases.

The Warburg impedance is the impedance due to slow diffusion. For a planar electrode in a large excess of electrolyte solution

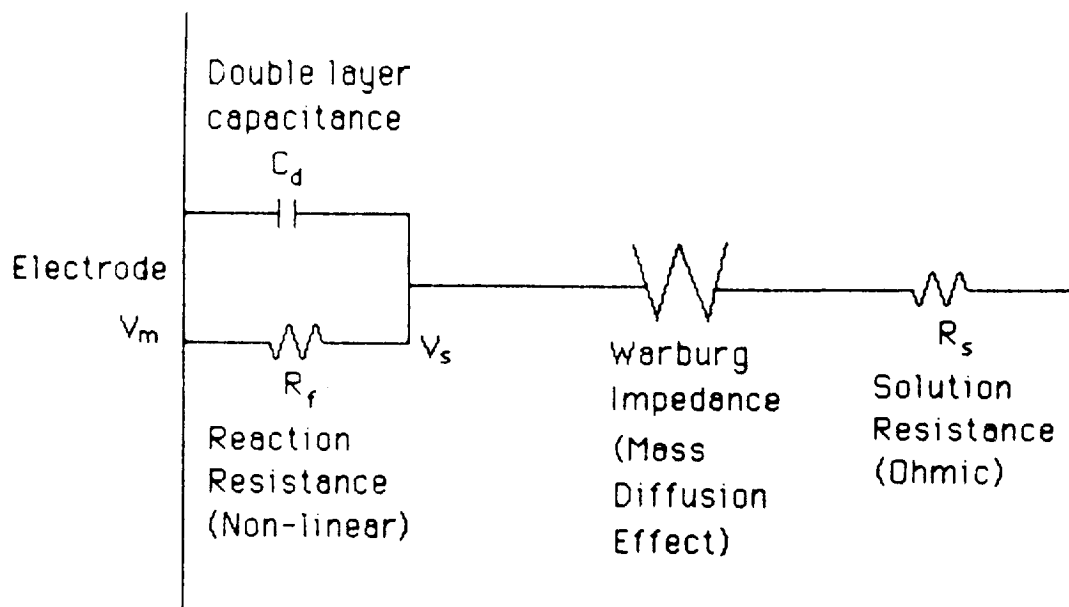


Figure 5. Equivalent circuit for electrode with capacitance, reaction, Warburg impedance and ohmic resistance.

$$Z_w \propto (j\omega D)^{-0.5} \quad (5)$$

The real and imaginary Warburg impedances are equal for this case. The Warburg impedance is usually manifested at frequencies less than 1 Hz. Measurements at frequencies as low as 0.0001 Hz have been reported. The period of such a measurement is about as long as a battery cycle, hence higher frequencies would be needed for state of charge determinations without substantially changing the state of charge.

Porous Electrodes

Most actual battery electrodes are high surface area porous electrodes. The electrode processes are distributed throughout the electrode volume instead of at a single surface. One porous electrode model is the idealized cylindrical pore shown in Figure 6. The pore walls are the solid surface where the electrode reaction and double layer charging occurs. At the electrode grid ($x=0$) all of the current is in the solid phase while at the electrode/separator boundary ($x=L$) all of the current is in the liquid phase. The current is transferred from the liquid to the solid along the pore wall.

Figure 7 shows the model circuit for the pore, which is often called a transmission line model. The impedance Z can include reaction, double layer capacitance and Warburg impedance. The impedance of the electrode, assuming a very large solid conductivity and no Warburg impedance is

$$Z_{\text{pore}} = \frac{\cosh(mL)}{km \sinh(mL)} \quad (7)$$

$$m^2 = \frac{a}{k} (R_f^{-1} + j\omega C_d)$$

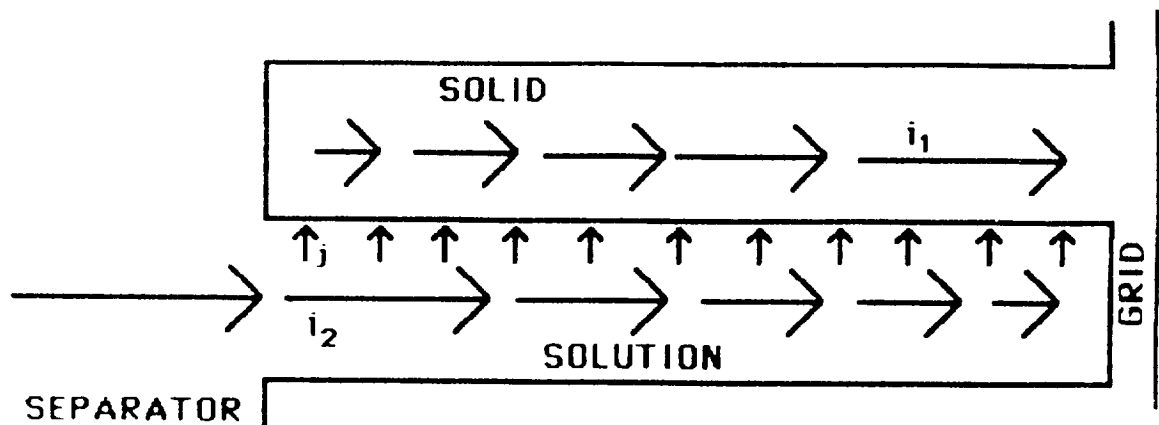


Figure 6. Idealized model of a cylindrical pore.

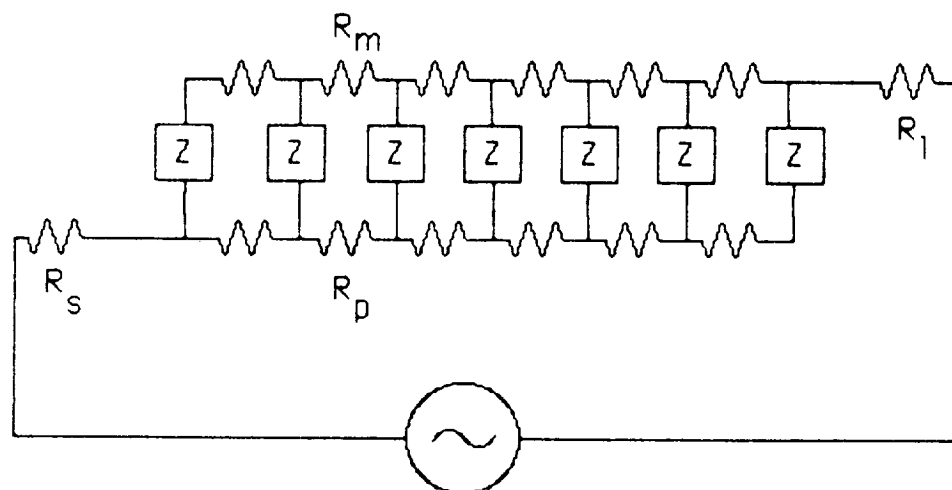


Figure 7. Equivalent circuit for the model in Figure 6.

This is a complicated expression to interpret, especially since m is a complex number, but it can be linearized for small values of mL , and the resulting expression is useful for estimating specific surface area. The important result is

$$\text{Im}(Z_{\text{pore}}) = \frac{awC_d L^3}{45 k^2}$$

Equation 8 is an approximation of Equation 7 that is valid at low frequencies, providing that the frequency is high enough that Warburg impedance is not a factor. A plot of $\text{Im}(Z)$ vs. frequency is linear in this range, and the specific area can be determined from the slope of the line.

EXPERIMENTAL

A three electrode cell was made by sandwiching a Cd electrode between two Ni electrodes. The electrodes were from an Eagle-Picher 50 A-Hr cell that had undergone destructive physical analysis. Separator material from the cell was used as separator in this cell. The cell was immersed in 31% KOH solution. A Ag/AgO reference electrode was placed in a separate compartment with 31% KOH. The two compartments were connected by a 1 mm Teflon tube filled with electrolyte, and the tube was placed near the Cd electrode at the center of the cell.

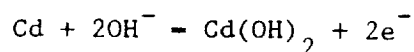
A EG&G/PAR model 363 potentiostat was used to control the potential between the Cd and reference electrode. A Wavetek signal generator supplied the voltage perturbations that were added to the D.C. offset voltage of the potentiostat. The potential and current monitors of the potentiostat were connected to a Tektronics storage oscilloscope, from which the peak current,

peak voltage and phase angles were obtained. Impedance spectra were obtained for GE 20 A-Hr cells using similar instrumentation. The reference electrode lead from the potentiostat was connected directly to the counter electrode terminal.

RESULTS

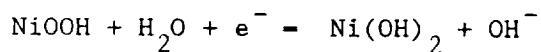
Eagle-Picher Electrodes

Figure 8 shows the experimental Nyquist plot for a charged and discharged Eagle Picher Cd electrode in a frequency range of 0.001 Hz on the right hand side to 1 Hz on the left hand side. The Warburg impedance dominated this part of the diagram, and it is much larger for the discharged electrode than the charged electrode. This can be explained by considering the electrode reaction



which produces $\text{Cd}(\text{OH})_2$ upon discharge. A solid film of reaction product would be a mass transfer barrier that would increase the electrode impedance.

Figure 9 shows the Nyquist diagram for the Ni electrode in the same frequency range as Figure 8. $\text{Re}(Z)$ is an order of magnitude smaller than for the Cd, while $\text{Im}(Z)$ is two orders of magnitude smaller. The primary mass transport process in the Ni electrode is thought to be proton (H) diffusion in the solid as the electrode reaction occurs:



Proton diffusion occurs rapidly since the hydrogen atom is small and easily moves between larger atoms in the solid lattice, hence the Warburg impedance of the Ni electrode is smaller. The curves for the charged and discharged electrodes are the same, indicating that a film does not grow during a cycle.

Eagle-Picher Cd Electrode

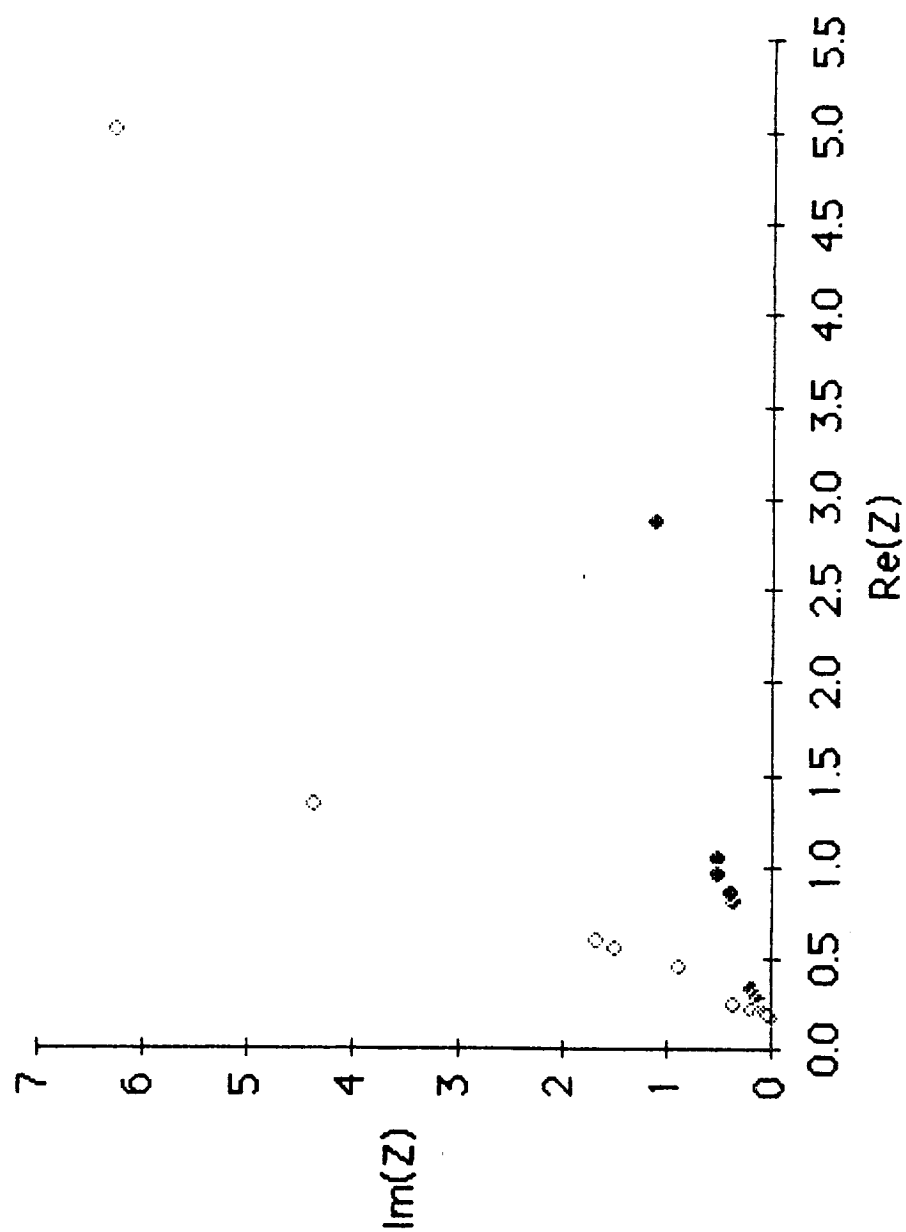


Figure 8. Nyquist plot for Eagle-Picher Cd electrode.

Eagle-Picher Ni Electrode

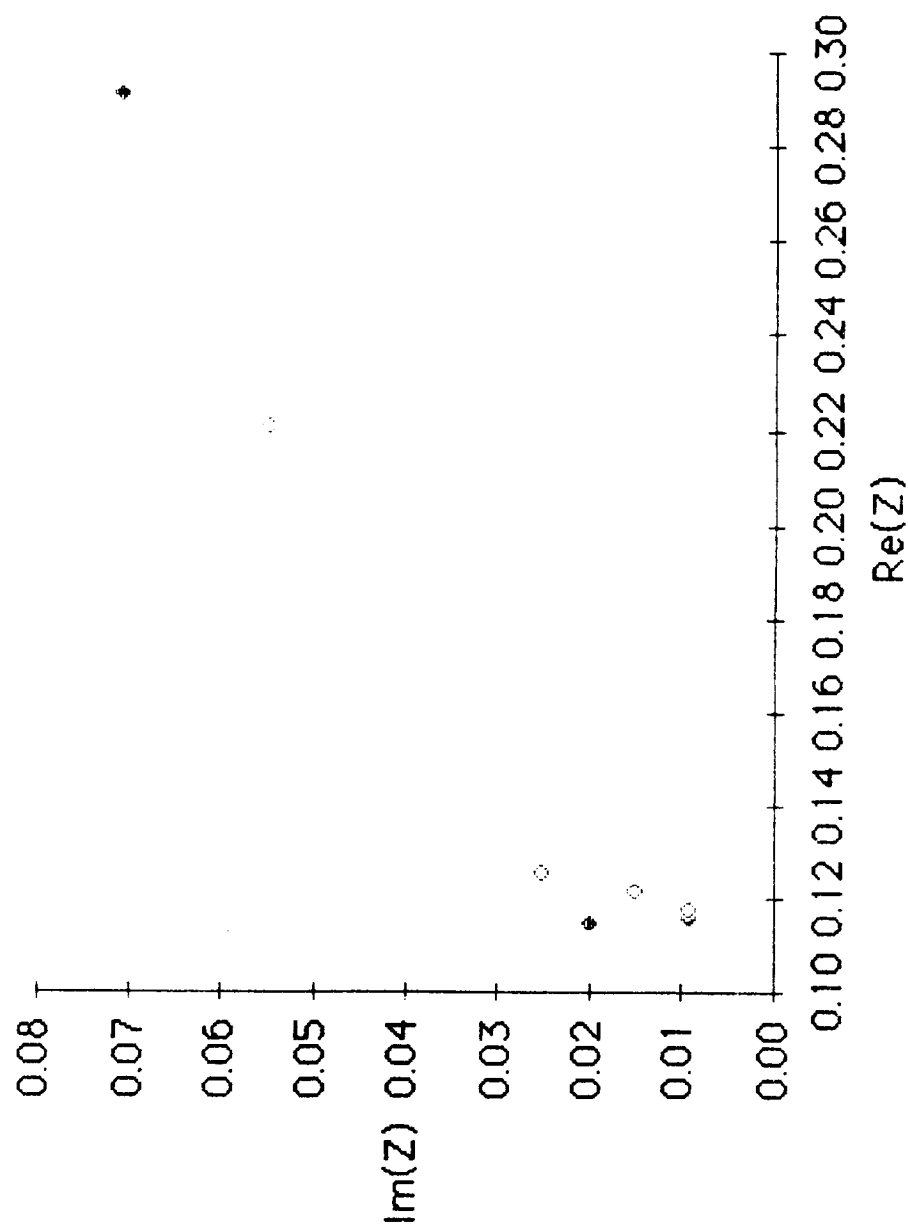


Figure 9. Nyquist plot for Eagle-Picher Ni electrode.

ORIGINAL PAGE IS
OF POOR QUALITY

Figure 10 shows a plot of $\text{Im}(Z)$ vs. frequency in a range from 100 - 3000 Hz for the Cd electrode. The plot is linear and the interfacial area can be estimated from the slope of the line. The double layer capacitance was assumed to be $80 \mu\text{F}/\text{cm}$ (Latham and Hampson, 1973), the electrode thickness was 0.04 cm, the solution conductivity $0.5 \text{ ohm}^{-1} \text{ cm}^{-1}$ and the effective conductivity in the porous electrode was estimated using the Bruggemann equation

$$k_{\text{eff}} = k(\text{porosity})^{1.5}$$

with a porosity of 0.25 to 0.3. The interfacial area was estimated to be 8 to $15 \text{ m}^2/\text{g}$, which compares with results of 2 to $50 \text{ m}^2/\text{g}$ determined by Pickett (1975) from BET (hydrogen adsorption) measurements. The BET technique determines total area, while the present technique measures only the electrochemically active area.

G.E. Cell

Some impedance spectra were measured for a G.E. 20 A-Hr cell. The cell had been on the shelf for about 14 years with the terminals shorted. It was cycled several times and a capacity of 21 A-Hr was obtained, however, the cell did not retain charge- it lost about half its capacity during overnight stand. The impedance spectra was measured in the low frequency range (0.001 to 1 Hz) in the following conditions: 1) discharged and overnight stand, 2) fresh charge, 3) fresh discharge, and 4) recharged and overnight stand. At 1 Hz the phase angle was zero, while at frequencies of about 100 Hz and larger the potential led rather than lagged the current, indicating that induction effects, which do not have an electrochemical explanation, dominated the capacitance effects.

Figure 11 compares the spectra of conditions 1 and 2. The impedance of the discharged cell is larger than the charged cell due to the $\text{Cd}(\text{OH})_2$ film

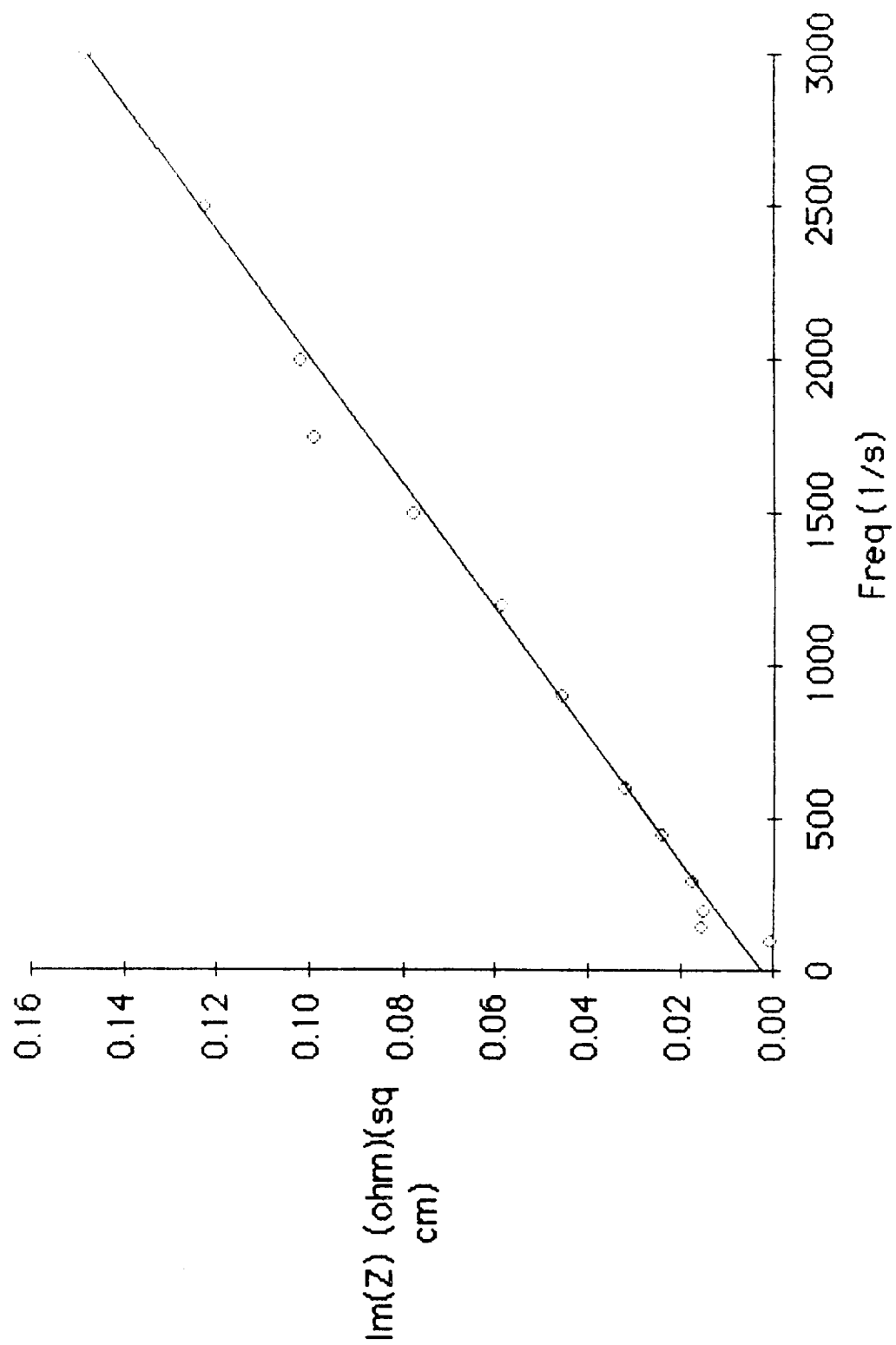


Figure 10. Imaginary impedance component vs. frequency for Eagle-Picher Cd electrode.

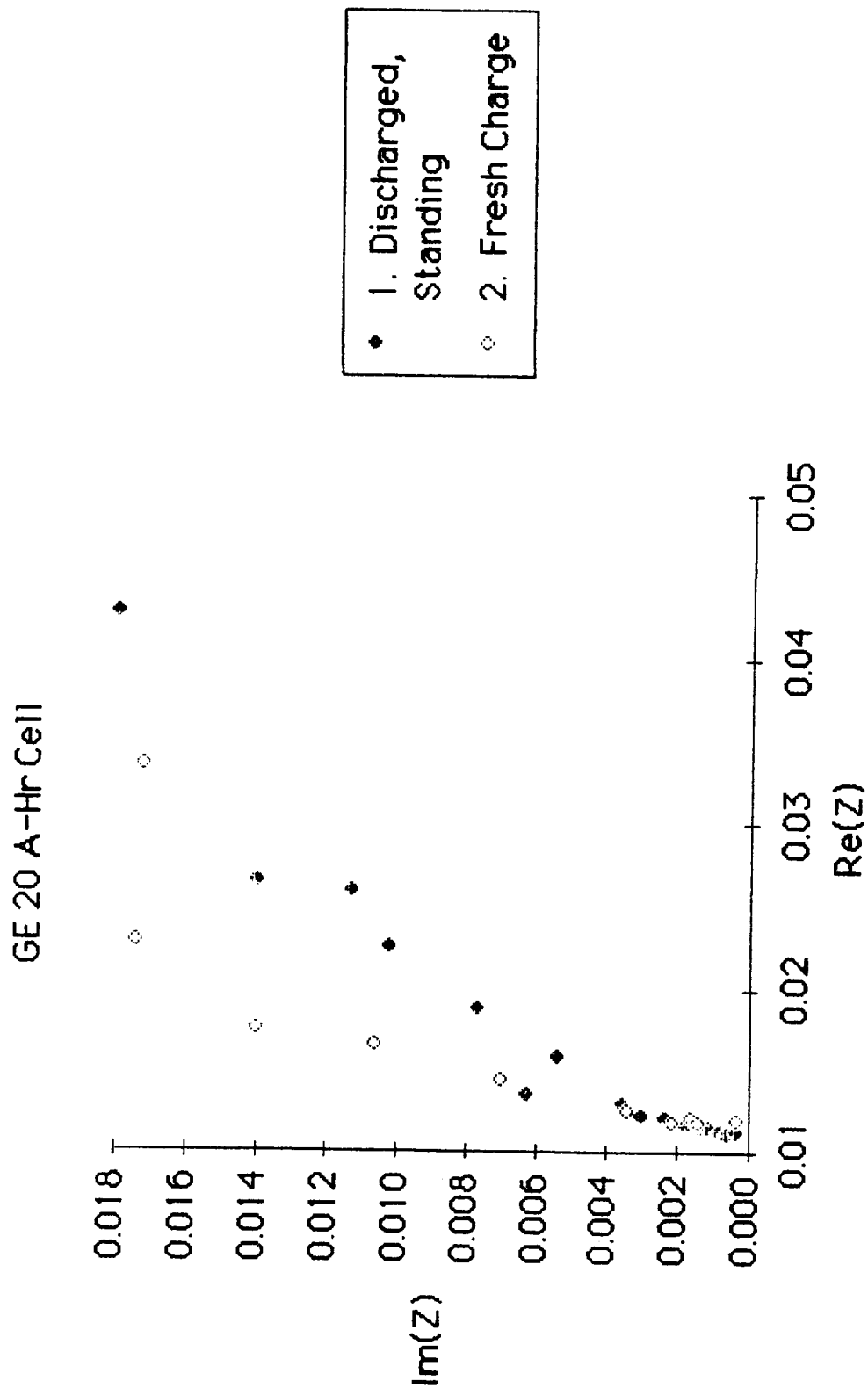


Figure 11. Nyquist plot for GE 20 A-Hr Cell.

that hinders diffusion. Figure 12 compares conditions 1 and 3, both of which are discharged conditions and yield similar spectra. Figure 13 compares the two recharged conditions, and there is a clear difference between the two results. The spectra for condition 4 are unlike the others observed. More data are needed to conclusively determine whether it is a bad set of measurements or if it represents reality. The dotted line shows how two humps, representing two time constants (one for each electrode) may be important. This would indicate that the recharged nickel electrode degrades upon stand.

CONCLUSIONS AND RECOMMENDATIONS

The following conclusions are made concerning this study: 1) the specific area of battery electrodes can be estimated using frequency response techniques during DPA. The results are consistent with those obtained by other workers. 2) Attempts to correlate cell state of charge are inconclusive. It seemed to work better for individual electrodes during DPA than for cells.

It is recommended that 1) methods for evaluating other electrode structural parameters such as porosity and tortuosity be developed, 2) a long term study of frequency response as a non-destructive battery test be undertaken. Ten weeks is insufficient time for such a study. The results of such a study would be a correlation of state of charge and of battery acceptability for space flight. 3) Develop quantitative data analysis of impedance in the low frequency (mass-transfer dominated) range. 4) Apply frequency response techniques outlined in this report to Ni/H₂ and Ag/Zn cells.

GE 20 A-Hr Cell

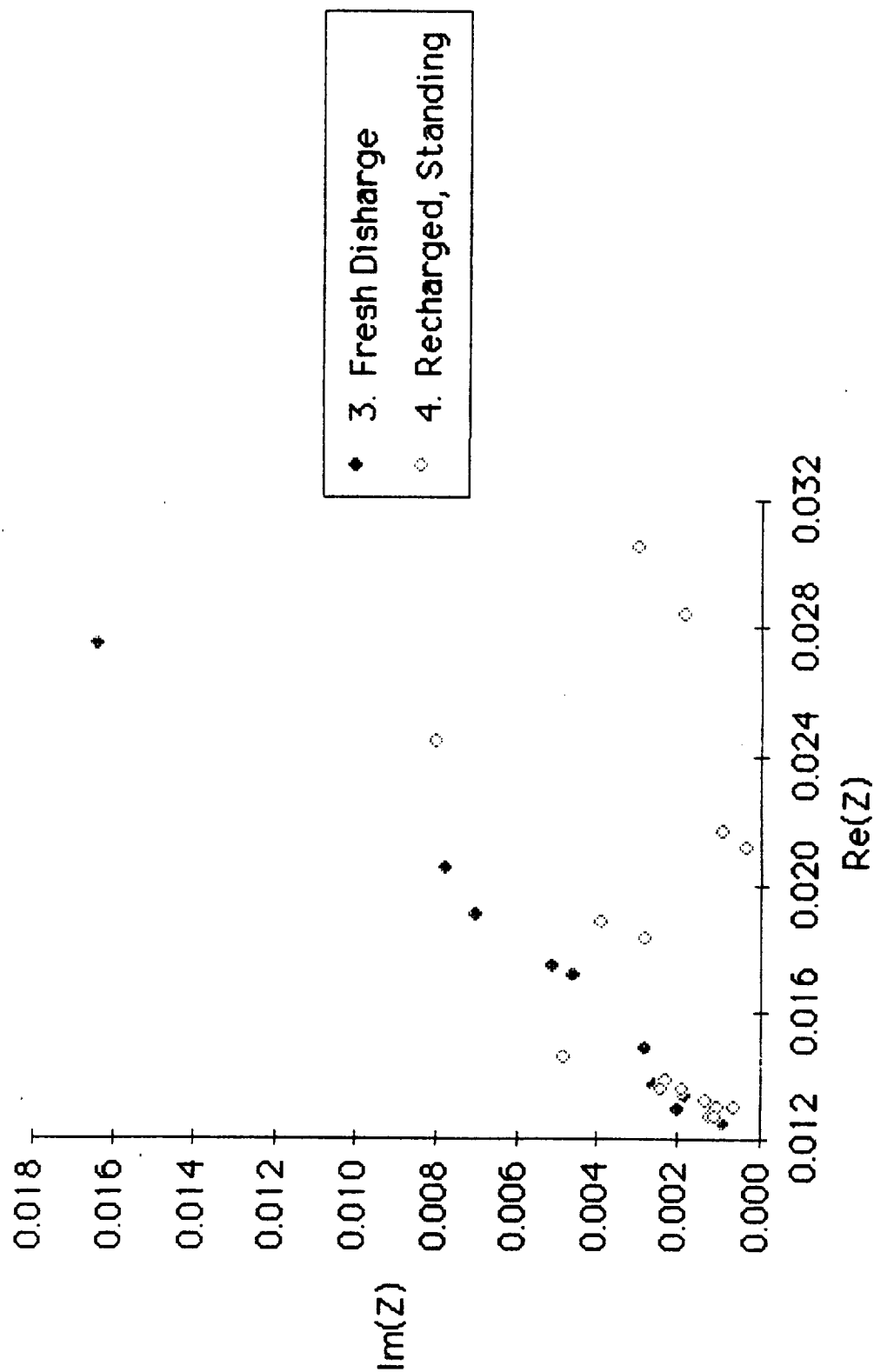


Figure 12. Nyquist Plot for G.E. 20 A-Hr cell (continued).

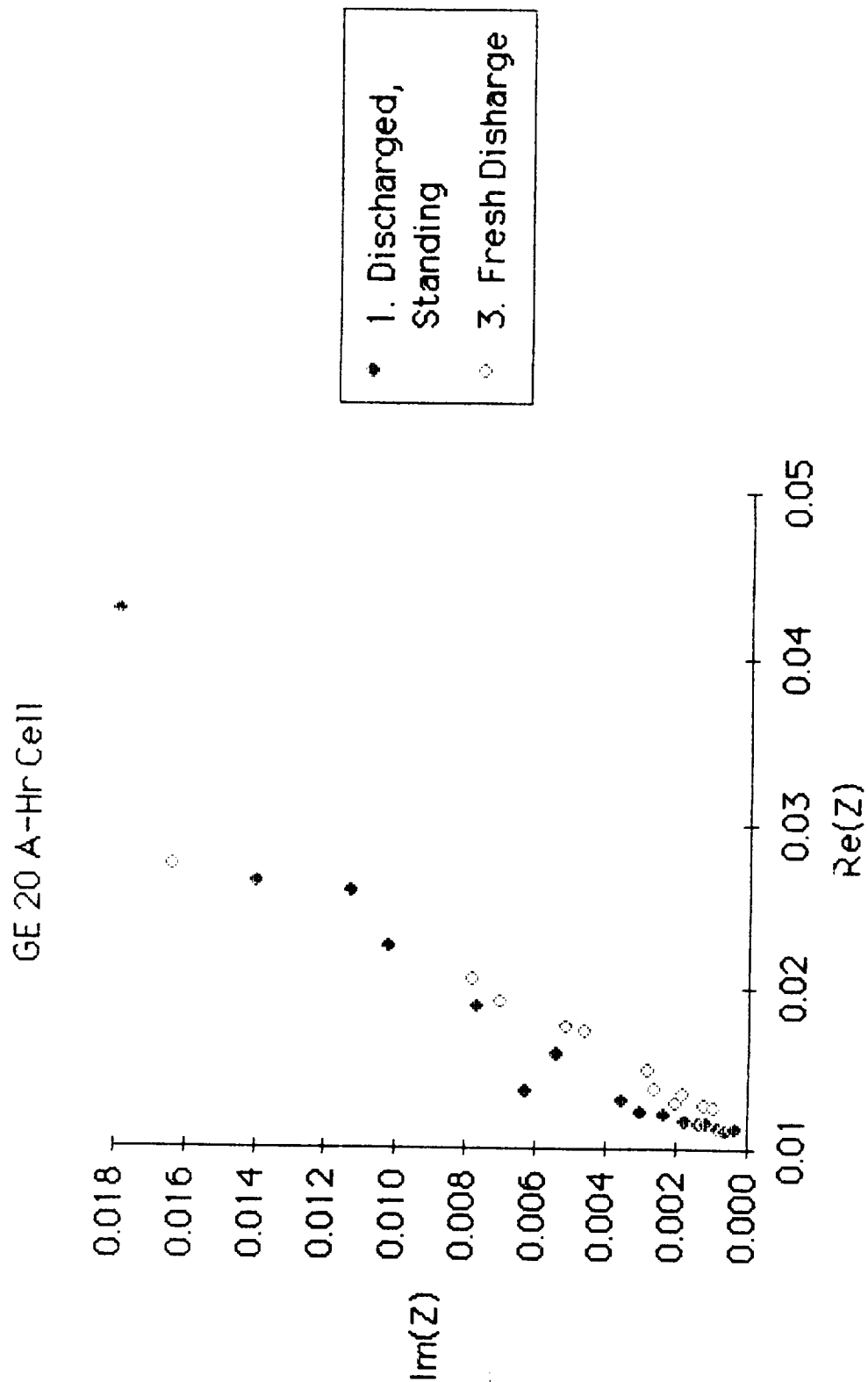


Figure 13. Nyquist plot of G.E. 20 A-Hr cell (continued).

REFERENCES

- R.D. Armstrong and K. Edmondson, Electroanal. Chem. and Interfac. Electrochem, vol 53, pp 371-387, 1974.
- R.D. Armstrong, K. Edmondson and J.A. Lee, J. Electroanal. Chem., vol 63, pp. 287-302, 1975.
- A.J. Bard and L.R. Faulkner, Electrochemical Methods, J. Wiley and Sons, New York, 1980.
- R.J. Brodd and H.J. DeWane, J. Electrochem. Soc., vol 110, p. 1091, 1963.
- R. Haak, C. Ogden and D. Tench, J. Power Sources, vol 12, pp 289-303, 1984.
- R.J. Latham and N.A. Hampson, in Encyclopedia of Electrochemistry of the Elements, vol 1, A.J. Bard, ed., Marcel Dekker, New York, 1973.
- J. Newman, Electrochemical Systems, Prentice Hall, Englewood Cliffs, NJ, 1973.
- D.F. Pickett, Air Force Aero. Propulsion Lab., Report No. AFL-TR-75-34, 1975.
- S. Sathyanarayana, S. Venugopalan and M.L. Gopikanth, J. Appl. Electrochem., vol 9, pp. 125-139, 1979.
- W. Tiedemann and J. Newman, J. Electrochem. Soc., vol 122, pp 70-74 1975.
- A.H. Zimmerman, M.R. Martinelli, M.C. Janecki and C.C. Badcock, ibid, pp. 289-298, 1982.